



# Potential model of a two-dimensional Bunsen flame

Bruno Denet

## ► To cite this version:

Bruno Denet. Potential model of a two-dimensional Bunsen flame. Physics of Fluids, 2002, 14(10), pp.3577-3583. 10.1063/1.1504448 . hal-00084901

**HAL Id: hal-00084901**

**<https://hal.science/hal-00084901>**

Submitted on 10 Jul 2006

**HAL** is a multi-disciplinary open access archive for the deposit and dissemination of scientific research documents, whether they are published or not. The documents may come from teaching and research institutions in France or abroad, or from public or private research centers.

L'archive ouverte pluridisciplinaire **HAL**, est destinée au dépôt et à la diffusion de documents scientifiques de niveau recherche, publiés ou non, émanant des établissements d'enseignement et de recherche français ou étrangers, des laboratoires publics ou privés.

## Potential model of a 2D Bunsen flame

Bruno Denet

IRPHE 49 rue Joliot Curie BP 146 Technopole de Chateau Gombert 13384 Marseille Cedex 13

France

submitted to Physics of Fluids

### Abstract

The Michelson Sivashinsky equation, which models the non linear dynamics of premixed flames, has been recently extended to describe oblique flames. This approach was extremely successful to describe the behavior on one side of the flame, but some qualitative effects involving the interaction of both sides of the front were left unexplained. We use here a potential flow model, first introduced by Frankel, to study numerically this configuration. Furthermore, this approach allows us to provide a physical explanation of the phenomena occurring in this geometry by means of an electrostatic analogy.

Keywords: laminar reacting flows

# 1 Introduction

The Michelson Sivashinsky equation [1] forms the basis of non linear descriptions of laminar premixed flames. While originally developed for the case of plane on average flames, variants of this equation have also been applied to spherical expanding flames [2] [3]. However, an extension of this equation valid for oblique flames has been obtained only recently by Joulin in [4] by adding a convective term to the original equation , which mimics the transverse velocity appearing as soon as the flame is maintained oblique compared to the direction of propagation. The motivation of this work can be found in the experimental setup of Truffaut and Searby [5], which the authors have called an inverted V flame. Actually this configuration is a sort of 2D Bunsen burner laminar flame, perturbed on one side by an applied electric field. A comparison of the model equation with the experiment has been remarkably successful, even from a quantitative point of view, and describes the development and saturation of wrinkles amplified by the Darrieus-Landau instability. However, this equation is limited to one side of the front. Searby and Truffaut have been able to exhibit an effect not described by the lagrangian Michelson Sivashinsky equation: when the flame is excited on one side, relatively small cells develop on this face of the flame but an overall curvature of the flame at large scale occurs.

This effect can only be explained by a model taking into account both sides of the flame. It turns out that such a model already exists in the form of an equation derived by Frankel [6]. We shall describe this model in more detail in section 2, but for the moment let us just say that the model assumes a potential flow both ahead and behind the flame, and consists of a boundary integral equation (the boundary is the flame front, seen as a discontinuity) involving electrostatic potentials. Some numerical simulations of this equation can be found in the literature [7] [8] [9] [10] in the case of expanding flames, but it has not been used for the moment in other geometries. We use here a slightly modified version of this equation to study the 2D Bunsen flame case. With this method, all the phenomena observed experimentally are recovered and it is possible to use an

electrostatic analogy in order to get a physical understanding of this problem.

In section 2 we present the Frankel equation in a form suitable to the present geometry and we take the opportunity to show that this equation naturally leads to a qualitative interpretation of the Darrieus Landau instability. In section 3 we present the results obtained in the 2D Bunsen flame configuration for various values of the parameters. Finally section 4 contains a conclusion.

## 2 Model

Let us first introduce some notations. We use two different flame velocities, the flame velocity relative to premixed gases  $u_l$  and the flame velocity relative to burned gases  $u_b$ . Without gas expansion caused by the exothermic reactions, these two different velocities would have the same value. However typically the density in burned gases is five to eight times lower than the density of fresh gases, which is the main cause of the Darrieus-Landau instability of premixed flames. If we define  $\rho_u$  the density of fresh gases,  $\rho_b$  the density of burnt gases,  $\gamma = \frac{\rho_u - \rho_b}{\rho_u}$  a parameter measuring gas expansion ( $\gamma = 0$  without exothermic reactions), then  $u_b = \frac{u_l}{1-\gamma}$  because of mass conservation. In many articles, the notion of flame velocity relative to burned gases is never used, however in the original Frankel paper, what is called flame velocity is actually  $u_b$ . We obtain below a Frankel equation relative to fresh gases, and this form of the equation will be simulated in the following section. The derivation closely parallels the original one, except for the flame velocity used and for the geometry. A sketch of the configuration can be found in Figure 1, the unburnt gases are injected at the velocity  $U$ . The flame has a shape typical of a Bunsen burner and propagates normally at a velocity  $u_l$  in the direction of unburnt gases. We also consider that  $U$  is constant in space and time and that the flame is attached at two constant position points.

The idea behind the Frankel equation is the following: the Michelson Sivashinsky equation is obtained as a development with  $\gamma$  as an expansion parameter. It has been shown in [11] that

at the lowest order in  $\gamma$ , the equation obtained by neglecting vorticity reduces to the Michelson Sivashinsky equation. So let us neglect vorticity everywhere, including in the burnt gases, we can define a velocity potential ( $w_u$  and  $w_b$  in the fresh and burnt gases), which is solution of the 2D Laplace equation:

$$w_{xx} + w_{yy} = 0$$

On the flame, which is a discontinuity in this formulation, the velocity potential has to satisfy

$$w_u = w_b$$

$$\left(-\frac{\partial w_b}{\partial n} + V - \vec{U} \cdot \vec{n}\right) \rho_b = \left(-\frac{\partial w_u}{\partial n} + V - \vec{U} \cdot \vec{n}\right) \rho_u$$

$$-\frac{\partial w_u}{\partial n} + V - \vec{U} \cdot \vec{n} = u_l + \varepsilon \kappa$$

$\kappa$  is the curvature at a given point on the flame ,  $\varepsilon$  is a constant number proportional to the Markstein length,  $\vec{n}$  is the normal vector at the current point on the front, in the direction of propagation. After some calculations, an evolution equation is obtained, valid for an arbitrary shape of the front (the reader is referred to [6] for more details on the derivation, please remember that the flame velocity used in this paper is  $u_b$  ).

$$V(\vec{r}, t) = u_l + \varepsilon \kappa + \vec{U} \cdot \vec{n} + \frac{1}{2} \frac{\gamma}{1 - \gamma} u_l - \frac{u_l}{2\pi} \frac{\gamma}{1 - \gamma} \int_S \frac{(\vec{\xi} - \vec{r}) \cdot \vec{n}}{|\vec{\xi} - \vec{r}|^2} dl_\xi + \vec{V}_{boundary} \cdot \vec{n} \quad (1)$$

This equation gives the value of the normal velocity  $V$  on the front as a sum of several terms, the laminar flame velocity with curvature corrections, the velocity of the incoming velocity field and an induced velocity field (all the terms where  $\gamma$  appears) which contains an integral over the whole shape (indicated by the subscript  $S$  in the integral ). This integral is a sum of electrostatic potentials.

Let us recall that, as is well-known, the formula for the induced velocity field at a position not located on the front is given by a different formula, which we shall use to reconstruct the velocity everywhere once the shape is known.

$$\vec{V}_{induced}(\vec{r}, t) = -\frac{u_l}{2\pi} \frac{\gamma}{1-\gamma} \int_S \frac{(\vec{\xi} - \vec{r})}{|\vec{\xi} - \vec{r}|^2} dl_\xi \quad (2)$$

i.e. compared to equation (1) the induced velocity term does not contain the constant term  $\frac{1}{2} \frac{\gamma}{1-\gamma} u_l$  . The last term  $V_{boundary}$  is a potential velocity field (continuous across the flame) added to the equation in order to satisfy the boundary conditions. Here the condition is simply that

$$(\vec{V}_{induced} + \vec{V}_{boundary}) \cdot \vec{n} = 0$$

at the injection location, where  $\vec{n}$  is parallel to  $\vec{U}$  , so that  $V_{boundary}$  is given by the same type of integral as  $V_{induced}$  , but over the image of the front, drawn as a dashed line in Figure 1.

Naturally, the shape evolves according to the velocity  $V(\vec{r}, t)$  :

$$\frac{d\vec{r}}{dt} = V \vec{n}$$

where  $\vec{r}$  denotes the position of the current point of the front.

We would like at this point to emphasize the analogy between the flame propagation problem and electrostatics. Let us consider a plane flame, infinite in the transverse direction. If we inject

fresh gases with a velocity equal to  $u_l$ , then the flame does not advance and the velocity in the burnt gases is  $u_b$  (left of Figure 2). As explained before we can add any potential velocity field which does not generate a jump of velocity across the flame (which is already described by  $V_{induced}$ ) so as to satisfy boundary conditions. In particular we can add a constant velocity field, which would show that if the velocity field in fresh gases is zero, the flame propagates at  $u_l$ , if the velocity field in the burnt gases is zero, the apparent flame propagation velocity is  $u_b$ . However equation (1) corresponds to the symmetrical situation depicted in the middle of Figure 2: the velocity field in the burnt and fresh gases has the same value (in the opposite direction)  $\frac{u_b - u_l}{2} = \frac{u_l}{2} \frac{\gamma}{1 - \gamma}$  (the constant value that appears in equation (1)) and the flame propagates at the apparent velocity  $\frac{u_b + u_l}{2}$ . There is an analogy of this situation with a uniformly charged infinite plane in electrostatics (Figure 2, right), which generates on both side an electric field of value  $\frac{\sigma}{2\epsilon_0}$  in the international system of units.

One of the purposes of this paper is to show that this analogy enables us to have a physical understanding of phenomena occurring in unstable premixed flames. Let us start in this section by showing that we can explain qualitatively the Darrieus-Landau instability. We consider once again an infinite plane flame. The induced velocity  $\frac{u_b - u_l}{2}$  just above the flame is simply obtained by integration over the whole front (left of Figure 3). Just on the front, the integral term in equation (1) vanishes because of symmetry reasons so that this term  $\frac{u_b - u_l}{2}$  has to be added explicitly in (1). Let us consider now a wrinkled flame (right of Figure 3). The induced velocity very close to the flame is obtained as before by integration over the whole front. However now we can see in the figure (point A) that a part of the integration produces a velocity in the direction opposite to the previous induced velocity field, which tends to amplify the existing wrinkle. A similar reasoning could be performed at point B, showing also an amplification. Furthermore, it is easily seen that smaller wavelengths lead to a higher instability, a known property of the Darrieus Landau instability when curvature effects are neglected. In conclusion of this paragraph, we can see that

the potential approximation leads to a physical explanation of the instability, which would be much more difficult to achieve for the complete problem.

Before presenting the results, we can note that an approach equivalent to the Frankel equation was used in [12] [13] [14] [15]; The idea leading to this equation was slightly different. In the Frankel case the idea was to generalize the Michelson Sivashinsky equation which had a lot of success for plane on average flames. Pinder and Talbot wanted to provide a complete numerical solution of the flame problem when the flame is seen as a discontinuity. When baroclinity is neglected we obtain exactly the Frankel equation problem, and it could be supplemented by resolutions with vortex methods in order to have a rigorous description of the velocity field (with creation of vorticity in the burnt gases). But this resolution is not very easy (i.e. not easier than a direct numerical resolution of the problem). In this article, in the spirit of the Michelson-Sivashinsky equation, and as in Ashurst's work (see for instance [9]), we keep the potential approximation for the 2D Bunsen flame case described in the introduction, and show that this description is qualitatively correct.

### 3 Results

In the Truffaut-Searby configuration that we try to model here, the 2D flame is perturbed on one side, close to the base of the flame, by an electrostatic apparatus. As a result, 2D wrinkles are created, with a wavelength depending on the frequency of the applied electric field, and propagate along the flame because of the tangential velocity. During their trip from the base to the tip of the flame, the perturbations are amplified by the Darrieus-Landau instability. A photograph of an experiment is given in Figure 4. The displacement of the cells during the exposure time can be seen, and gives an idea of the dynamics of the flame. A successful description of the phenomena described above has been given by a Lagrangian Michelson-Sivashinsky equation in [4]. However this approach is inherently limited to one side of the flame, and cannot describe



phenomena involving interaction of both sides, such as the large scale curvature of the flame that can be observed in Figure 4.

We use here the Frankel equation [1] to study this problem. Let us first verify that we are able to recover the experimental results with this model. We excite the flame by applying a velocity  $v_x = a \cos(\omega t)$  at the fourth point starting from the bottom of the flame,  $x$  is the direction perpendicular to the injection velocity. As the flame front is described by a chain of markers (technical details on the numerical method can be found in [10]) the position of this point is not strictly constant, but the perturbations being small at this location, we have found that this type of forcing is satisfactory i.e. it generates a well defined wavelength related to the frequency and the tangential velocity. Figure 5 is obtained by a numerical simulation for parameters  $U = 10$   $L = 4$   $\varepsilon = 0.2$   $a = 1$   $\gamma = 0.8$   $\omega = 50$  ( $L$  is the distance at the base of the flame, in all the calculations  $u_l = 1$ ). The number of markers used in the simulation is not constant in time but is typically around 900. On this figure are plotted both the shape of the front and the induced velocity field (actually  $V_{induced} + V_{boundary}$ , see equation (2)). Arrows very close to the front are not drawn in this figure, as the formula for the induced velocity field cannot be applied when the distance from the front is of the order of the distance between successive markers. Naturally the analogy with Figure 4 is striking: both the wrinkle amplification and subsequent saturation by non linear effects are observed, but also the large scale curvature (i.e. as we get closer to the tip, the side opposite to the forcing gets more and more deflected). This progressive deviation of the right side of the flame is a consequence of the induced velocity field, which has a component towards the right when one approaches the tip, as can be seen in Figure 5.

This large scale deviation was observed by Truffaut and Searby, and for the moment the Frankel equation succeeds in producing this effect. But a qualitative interpretation can also be obtained. We have seen that it can be considered that the induced velocity is caused by a uniformly positively charged front (the electrostatic analogy). As the wrinkle develops when we get closer to the tip,

the velocity has a sinusoidal component with the wrinkle wavelength in the direction parallel to the front, and, as a solution of a Laplace equation, this component decays exponentially in the perpendicular direction. So, the perturbation with the wrinkle wavelength will be small on the side opposite to the forcing. Sufficiently far, the perturbed side can just be considered as a straight unperturbed line, but with a charge higher than before (a consequence of the Gauss theorem: the charge inside a small rectangle is higher because of the wrinkle). So the situation is close to the sketch of Figure 6. At the base of the flame, the charge is the same for both sides of the flame. As a result the velocities induced by both sides of the flame have the same absolute value, but are in the opposite direction if we consider for simplicity both sides parallel. The total induced velocity field nearly cancels in the fresh gases, and is high in the burnt gases. On the contrary, in a zone with well-developed wrinkles, the charge is higher on the wrinkled side because of the previous argument, and generates a velocity with a higher absolute value. The total induced velocity field is thus directed towards the right, and tends to cause a deviation of both sides of the flame (see Figure 5). There is also the fact that the front cannot be considered infinite close to the tip, which generates a velocity upward because there is no compensation of the upward velocity field created by the charges below (on the other hand, at the base of the flame the velocity is very small because the downward  $V_{induced}$  is compensated by  $V_{boundary}$  which is a velocity field created by the image of the flame: see Figure 1).

The potential flow model is thus in very good qualitative agreement with the experiments of Searby and Truffaut. However, it does not seem possible to obtain the same quantitative agreement for the development of a wrinkle on one side, as in the lagrangian Michelson Sivashinsky case [4]. The reason can be understood in the following way : actually the results of [4] are obtained by a Michelson Sivashinsky equation with modified coefficients. The dispersion relation is fitted in order to be in agreement with the experimental results, then there is also a modification (compatible with an expansion in  $\gamma$ ) of the coefficient of the non linear term. With these modifications the

development of perturbations along the front can be described quantitatively. However in our case a modification of the coefficients to fit the dispersion relation would have also an effect on the other side on the front. It seems unlikely that the same set of coefficients can describe precisely both the dispersion relation and the effect of one side on the other, although some kind of compromise can perhaps be found.

So we will limit ourselves in this paper to qualitative results obtained by the Frankel equation. A positive point of this model is that we can vary easily the physical parameters, contrary to experiments. Of course changing the width at the base of the flame involves a whole new burner, but it is also difficult experimentally to increase the injection velocity, because the flame has to be anchored on the rod where the electric field is applied.

When perturbations of the 2D Bunsen flame do exist on both sides of the front, the question arises of knowing the type of modes that will develop, sinuous or varicous. It is possible to impose one of this mode by applying an electric field on both sides, with a well-defined phase relationship, but we prefer here to study what will happen naturally. We apply now a white noise at the base of the flame, at the same location as before, but on both sides. A typical front shape, for a small width  $L = 1$  and a large injection velocity  $U = 40$  is shown in Figure 7. The other parameters are  $\varepsilon = 0.2$  and  $\gamma = 0.8$ , the amplitude of the white noise being  $a = 5$ ,  $v_x = a(random - 0.5)$  where *random* is a random number (uniform distribution between 0 and 1), always imposed on the fourth point from the base of the flame. The number of points used in the simulation is typically 7000. The main conclusion of different calculations, which can be seen on the Figure, is the following: in a first stage, perturbations develop on both sides in an independent way, neither the sinuous nor the varicous mode are favored. However, for a sufficient length of the flame, close to the tip, the sinuous mode is the dominant one. The sinuous zone corresponds to a distance between both sides of the order of the wavelength, which is natural for a potential model. Actually, when this distance is comparable to the wavelength, the perturbations have the following choice: be damped

because they do not have a sufficient distance to develop, or amplify as before but in a sinuous mode. A similar sinuous mode has been obtained in [16] for twin flames in stagnation point flows.

Another interesting problem is the wavelength itself. For a planar on average flame without gravity, perturbations with the most amplified wavelength emerge from a flat front, then non linear effects come into play, cells merge and in the end only one cell remains. This effect is generally not observed in oblique flames, simply because the available length is too short, and the wrinkles reach the tip before merging. In order to observe the merging (in a lagrangian way) we consider a very large flame:  $U = 10$   $L = 20$   $\varepsilon = 0.2$   $\gamma = 0.8$ . These conditions correspond either to a very large flame at atmospheric pressure or to a flame at high pressure. We start the simulation from a flame which has been submitted for some time to a white noise everywhere, not only at the base, as in Figure 7. This front can be seen in Figure 8 which will be used as an initial condition. The small cells of this flame evolve in the Figures 9 to 11 without any noise. The merging of the cells, similar to the one observed in planar on average flame, appears, but occurs here in a lagrangian way, as the cells are convected towards the tip. The reader can find a similar behavior obtained recently with the lagrangian Michelson Sivashinsky equation in [17] (see also the corresponding animation which can be found on the Combustion Theory and Modelling web site). The effect seen previously exists also here, sinuous modes dominate at the tip. However as the perturbations develop, the overall surface being more or less constant, the height of the flame becomes smaller, as seen in Figure 11. The same effect is observed in turbulent flows, and as the available length on each side of the mean flame is smaller, the merging of cells becomes more difficult. An example of turbulent flames obtained in this configuration, which are relatively similar to the solutions obtained here in the presence of noise, can be found in [18].

After this solution, we have not seen a continuation of the merging process, on the contrary new cells appear on the front while some cells merge. Also we have seen no sign that the flame will ultimately recover its unperturbed shape. The two last observations are related to the level of

numerical noise present in the simulation, for instance insertion and deletion of markers. Actually we have found in another oblique configuration (V flame with initial perturbations) and for similar sizes, that it is possible to recover a more or less stationary flame by using twice as many markers in the simulation. In [4], it has been suggested that for a sufficient injection velocity (i.e. in normal situations), the instability of the flame is convective, which seems to be the case with the potential model used here. However, just as in the expanding flame case, it appears that for large sizes, the flame is extremely sensitive to any external noise. Very small injection velocities, corresponding to an absolute instability, could actually lead to flashback. We have seen some indications that this phenomenon actually occurs, but it was not possible to describe correctly the evolution with the current algorithm after the flame enters the tube.

## 4 Conclusion

In this article, we have studied the 2D Bunsen flame configuration proposed by Truffaut and Searby by means of a model equation which considers the flow as potential both ahead and behind the flame. It has been shown that this approximation gives a good qualitative description of the phenomena observed. On the other hand, it is probably difficult to obtain a complete quantitative agreement with experiments with this model, contrary to modified versions of the Michelson-Sivashinsky equation, which do not describe the repulsion effect of the perturbed side of the front. We expect however that other oblique flame geometries can be studied with this approach, such as V flames or 3D premixed Bunsen burner flames. However the 3D case is very difficult technically, because the treatment of reconnections implemented here in 2D is challenging in 3D (it is ironic that these reconnections occurring close to the tip play a minor role in the physics, except for symmetrical forcings, but are the main numerical difficulty of the problem). Another natural extension of this work would be to consider a flame in a turbulent flow, in order to get an estimate

of the relative importance of turbulence and of the Darrieus-Landau instability. The author has already done some work with turbulence and hydrodynamic instability for expanding flames, but this could now be extended to oblique flames. We have also found in this article that the qualitative behavior can be different for flames in different geometries. This effect is known in laminar flame configurations, but certainly deserves attention also in the turbulent case.

**Acknowledgments:** the author would like to thank J.M. Truffaut, G. Searby and G. Joulin for helpful discussions, and for the photograph included in this article.

## References

- [1] G.I. Sivashinsky. Nonlinear analysis of hydrodynamic instability in laminar flames: Part 1: derivation of basic equations. *Acta Astronautica*, 4:1117, 1977.
- [2] Y. D'Angelo, G. Joulin, and G. Boury. On model evolution equations for the whole surface of three-dimensional expanding wrinkled premixed flames. *Combust. Theory Modelling*, 4:317, 2000.
- [3] L. Filyand, G.I. Sivashinsky, and M.L. Frankel. On the self-acceleration of outward propagating wrinkled flames. *Physica D*, 72:110, 1994.
- [4] G. Searby, J.M. Truffaut, and G. Joulin. Comparison of experiments and a non linear model equation for spatially developing flame instability. *Physics of Fluids*, 13(11):3270, 2001.
- [5] J.M. Truffaut and G. Searby. Experimental study of the Darrieus-Landau instability of an inverted V flame, and measurement of the Markstein number. *Combust Sci. Tech.*, 149:35, 1999.
- [6] M.L. Frankel. An equation of surface dynamics modeling flame fronts as density discontinuities in potential flows. *Phys. Fluids A*, 2(10):1879, 1990.

- [7] M.L. Frankel and G.I. Sivashinsky. Fingering instability in nonadiabatic low Lewis number flames. *Phys. Rev. E*, 52(6):6154, 1995.
- [8] S.I. Blinnikov and P. V. Sasorov. Landau Darrieus instability and the fractal dimension of flame fronts. *Phys. Rev. E*, 53(5):4827, 1996.
- [9] W.T. Ashurst. Darrieus-Landau instability, growing cycloids and expanding flame acceleration. *Combust. Theory Modelling*, 1:405, 1997.
- [10] B. Denet. Frankel equation for turbulent flames in the presence of a hydrodynamic instability. *Phys. Rev. E*, 55(6):6911, 1997.
- [11] G.I. Sivashinsky and P. Clavin. On the non linear theory of hydrodynamic instability in flames. *J. Phys. France*, 48:193, 1987.
- [12] M.Z. Pindera and L. Talbot. Flame induced vorticity: the effects of stretch. *Proc. Combust. Inst.*, 21:1357, 1986.
- [13] W.T. Ashurst. Vortex simulation of unsteady wrinkled laminar flames. *Combust. Sci. Tech.*, 52:325, 1987.
- [14] M.Z. Pindera and L. Talbot. Some fluid dynamic considerations in the modeling of flames. *Combust. Flame*, 73:111, 1988.
- [15] C.W. Rhee, L. Talbot, and J.A. Sethian. Dynamical behaviour of a premixed turbulent open v flame. *J. Fluid Mech.*, 300:87, 1995.
- [16] G. Joulin and G.I. Sivashinsky. On the non linear hydrodynamic stability and response of premixed flames in stagnation-point flows. *Proc. Combustion Institute*, 24:37, 1992.
- [17] G. Boury and G. Joulin. Nonlinear response of premixed flame fronts to localized random forcing in the presence of a strong tangential blowing. *Combust. Theory Modelling*, 6:243, 2002.

- [18] H. Kobayashi, T. Tamura, K. Maruta, T. Niioka, and F.A. Williams. Burning velocity of turbulent premixed flames in a high-pressure environment. *Proc. Combustion Institute*, 26:389, 1996.

## List of Figures

Figure 1 : Configuration. Solid line: flame front, dashed line: electrostatic image of the front

Figure 2: Left: flame stabilized because of the velocity  $u_l$  in the fresh gases. Middle: flame seen in a reference frame with symmetrical velocities in burnt and fresh gases. Right: electrostatic analogy with a uniformly charged plane

Figure 3: A qualitative explanation of the Darrieus-Landau instability : comparison of a plane and a wrinkled flame. Effect of nearby points on the propagation velocity.

Figure 4: Photograph of an experimental 2D Bunsen flame submitted to a sinusoidal forcing on one side (courtesy of J.M Truffaut and G. Searby)

Figure 5: A flame obtained numerically for a sinusoidal forcing on one side with the associated induced flow field (including the flow field of the image front). Parameters  $U = 10$   $L = 4$   $\varepsilon = 0.2$   $a = 1$   $\gamma = 0.8$   $\omega = 50$

Figure 6: A qualitative explanation of the deviation observed in the previous figure. Because of Gauss theorem, the perturbed flame can be seen sufficiently far as a plane with a higher charge.

Figure 7: Flame excited on both sides close to the base by a white noise. Parameters  $L = 1$   $U = 40$   $\varepsilon = 0.2$  and  $\gamma = 0.8$ , the amplitude of the white noise being  $a = 5$

Figure 8: Initial condition for a simulation with a large domain. The development of the perturbations can be seen in the next figures. Parameters  $U = 10$   $L = 20$   $\varepsilon = 0.2$   $\gamma = 0.8$

Figure 9: Development of the instability for the initial condition given in Figure 8.

Figure 10: Development of the instability for the initial condition given in Figure 8



Figure 11: Development of the instability for the initial condition given in Figure 8

Figure 1: Denet, Phys. Fluids

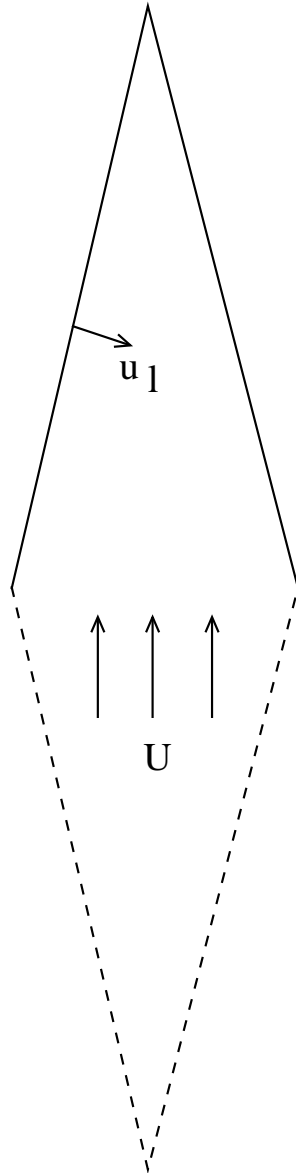


Figure 2: Denet, Phys. Fluids

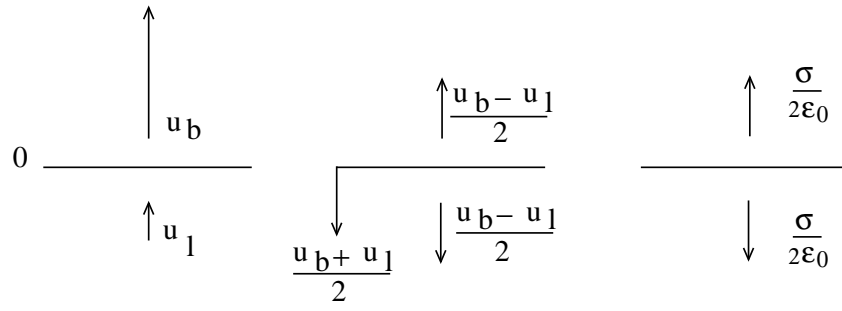
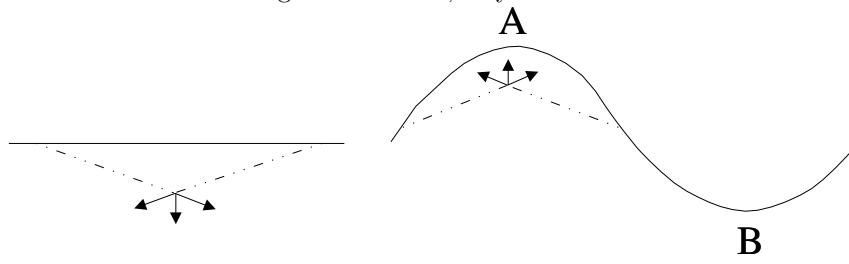


Figure 3: Denet, Phys. Fluids



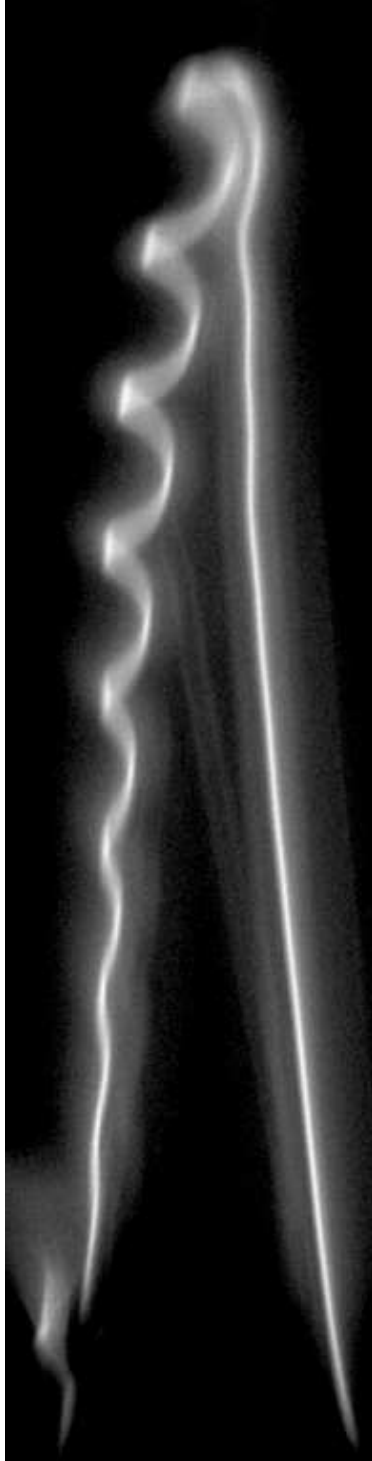


Figure 5: Denet, Phys. Fluids

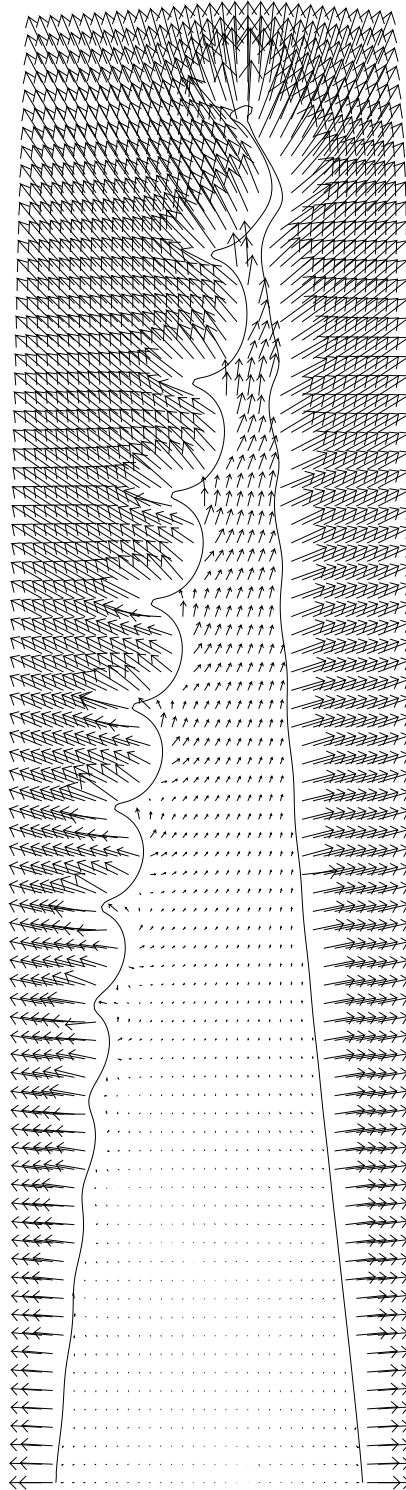


Figure 6: Denet, Phys. Fluids

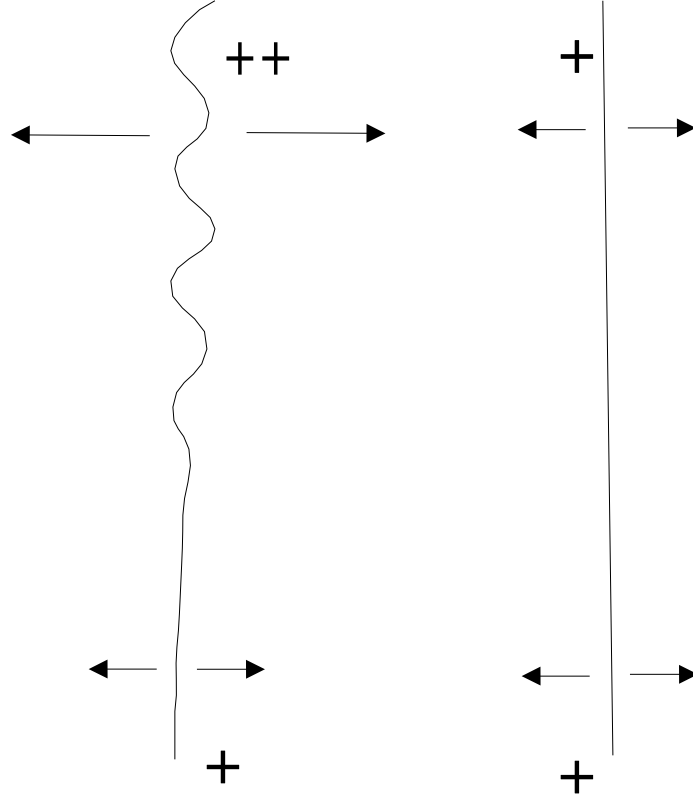


Figure 7: Denet, Phys. Fluids





Figure 8: Denet, Phys. Fluids

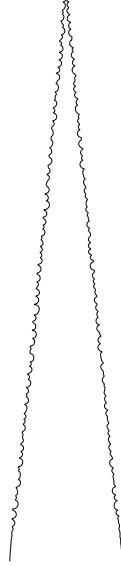


Figure 9: Denet, Phys. Fluids

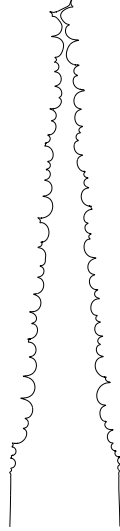


Figure 10: Denet, Phys. Fluids

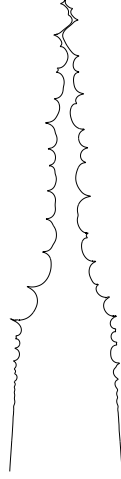


Figure 11: Denet, Phys. Fluids

